EVALUATION OF METHODS FOR DETERMINING DEMAND-LIMITING SETPOINT TRAJECTORIES IN COMMERCIAL BUILDINGS USING SHORT-TERM DATA ANALYSIS

Kyoung-ho Lee and James E. Braun
Ray W. Herrick Laboratories, School of Mechanical Engineering
Purdue University, West Lafayette, IN
leekh@purdue.edu and jbraun@purdue.edu

ABSTRACT

This paper presents the evaluation of three different methods for determining zone temperature setpoint variations that limit peak electrical demand in buildings. The methods were developed in a companion paper (Lee and Braun 2006b) and are evaluated in the current paper through simulation for two different buildings. One of the buildings houses the Iowa Energy Center and is representative of a small commercial building. This building was modeled using a detailed inverse model that was developed in a previous study. The other building is the Santa Rosa Federal building, which is representative of a large commercial building. This building was modeled using Energy Plus, which was calibrated using test data. All three methods worked well in terms of peak demand reduction. In addition, two of the methods provided good predictions of peak load reduction for both buildings.

INTRODUCTION

It is possible to achieve significant reductions in peak cooling loads for buildings by making use of the structural thermal mass through adjustments in zone temperature setpoints within the limits of comfort. The thermostat settings are lowered prior to the demand-limiting period and then adjusted upwards in an optimal way to minimize peak demand. A companion paper by Lee and Braun (2006b) develops three simplified demand-limiting methods, termed the SA (semi-analytical), ESA (exponential setpoint equation-based SA), and WA (weighted-averaging) methods, that determine zone temperature setpoint trajectories that attempt to minimize peak demand. The SA and ESA methods employ simple inverse building models trained with short-term data and use analytical solutions from the models for the setpoint trajectories. The WA method exploits a locally linear relation between zone temperature and cooling loads. The setpoint trajectory that minimizes the peak cooling load is estimated through a weighted averaging of two control setpoint trajectories which should produce load variations that intersect at some point during the on-peak period. The simple methods do not require measurements of solar radiation and only require one or two days of hourly data for outdoor temperatures and cooling loads.

The primary purpose of the current paper is to evaluate the performance of the simplified demand-limiting methods. A simulation study was performed for two buildings representative of a small and large commercial application. A detailed discussion of the simuation and its results are presented in the following sections.

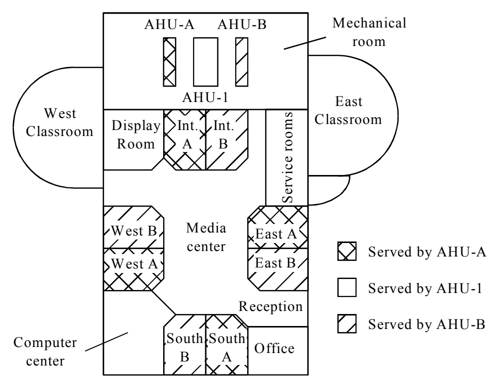

Figure 1 Schematic diagram of floor plan for the ERS

DESCRIPTION OF BUILDINGS

ERS Building

The Iowa Energy Center Engineering Resource Station (ERS) building is typical of small commercial buildings that employ packaged air conditioning equipment. It is a single-story building having a slab floor and is located in Ankeny, Iowa. The ERS is a demonstration and test facility built to compare different energy-efficient measures, to record energy consumption, and to disseminate information concerning energy-efficient design and operation of buildings. A schematic diagram of the floor plan for the ERS is shown in Figure 1. Each test room has 275 ft^2 of floor area with a ceiling height of 8.5 ft. The height of plenum zones above the test zones is 5.5 ft. The test room zones within a pair are identical and labeled 'A' and 'B'. Power densities for lighting and electric equipment are 2.2 and 3.4 W/ft^2. Detailed descriptions of the building were presented by Lee and Braun (2004, 2006a)

Santa Rosa Federal building

The Santa Rosa Federal building is a medium-sized governmental office building located in Santa Rosa, CA (Xu et al. 2006). The floor area is around 80,000 ft^2 and is composed of two spaces for offices and courtrooms, which are separated. The office area is located to the west of the space for courtrooms. It has three stories with moderate structural mass, having 6" concrete floors and 4" exterior concrete walls. The office area has a medium furniture density and standard commercial carpet on the floor. The window-to-wall ratio of the building is 0.67, with floor-to-ceiling glazing on the north and south façades and significantly smaller glazing fractions on the east and west. The windows have single-pane tinted glazing. The internal lighting and electric equipment gains for the Santa Rosa building model are approximately 0.2 and 0.3 W/sq-ft, respectively. The total number of occupants in the office areas is approximately 100 (400 ft^2/person).

DESCRIPTION OF BUILDING MODELS

Inverse Model for ERS

All test zones (West, East, South, and Interior) for the ERS were modeled as a single zone using an inverse model described by Lee and Braun (2004, 2006a). Each of the walls uses two capacitors to represent the mass of the walls and three resistors to represent the wall coupling to the ambient, the conduction within the wall and the wall coupling to the zone. The inverse building model was tuned with test data from 2001 and 2004. The total number of days for model training was 35 days. These days included night setup, load-shifting, and demand-limiting control strategies operated over a range of weather conditions. The integrated RMS (root-mean-squared) error of the building model for training was 7.27% for cooling load prediction. Figure 2 shows a comparison of predicted and actual cooling loads for a single day.

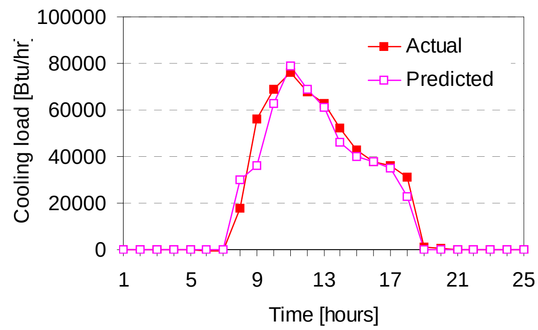

Figure 2 Testing of trained inverse model for ERS building.

EnergyPlus Model for Santa Rosa Building

An EnergyPlus (US DOE 2005) model was developed for the Santa Rosa building that follows the mechanical system layout. (Xu et al. 2006) The building interior spaces were divided into six zones, two zones per floor. The geometry of the model is shown in the Figure 3. The lighting power density and electric equipment load were estimated by inspections of the building, which are 0.2 and 0.3 W/ft^2, respectively. One large capacity chiller having variable speed was used to model the behavior of the three chillers having staged controls. The cooling plant was oversized to a similar extent as in the real building.

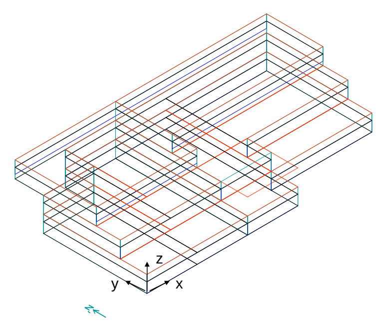

Figure 3 Three-dimensional diagram of Santa Rosa Federal building

Tuning of the model was conducted by comparing simulated chiller power to measured power and primarily adjusting window shading. From a detailed inspection of the geometry around the windows, it was found that the location of the window glass was receded towards the inside surface of exterior walls. This receding results in a shading effect that was added to the simulation. Fine tuning was performed by changing the internal mass surface area and ventilation flow rate within reasonable bounds.

Calibration of the model was performed by comparing simulated chiller power with actual chiller power measured for some hot days in 2004. Figure 4 compares measured outdoor temperatures for two selected days in 2004. The measured outdoor temperatures were used as input outdoor temperatures for the building model simulation. Since no other ambient conditions, such as solar radiation were available for the building, TMY data for San Francisco was used instead. However, simulation results indicate that the chiller power is relatively insensitive to sky conditions for this building and time of year. The setpoint schedules that were employed on the two days and used in the calibration runs are represented in Figure 5.

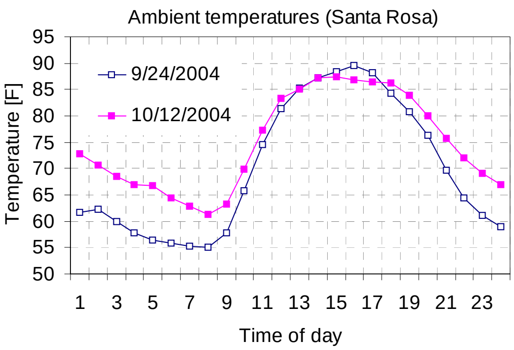

Figure 4 Outdoor temperatures for two test days in 2004 at the Santa Rosa building

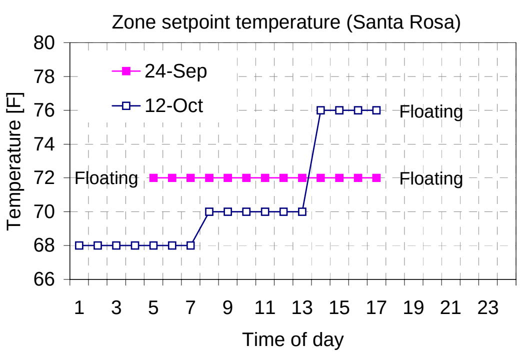

Figure 5 Precooling and demand-limiting setpoint schedules used in 2004 testing at Santa Rosa building

The simulated and measured chiller powers are compared in Figure 6 and Figure 7. The simulated chiller power has a similar magnitude and variation as the actual chiller power. The results from the building model simulation are in relatively good agreement with the measured data.

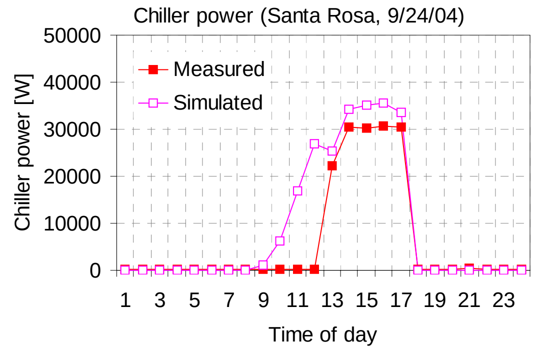

Figure 6 Comparison of simulated and actual chiller power on 9/24/04 for Santa Rosa building

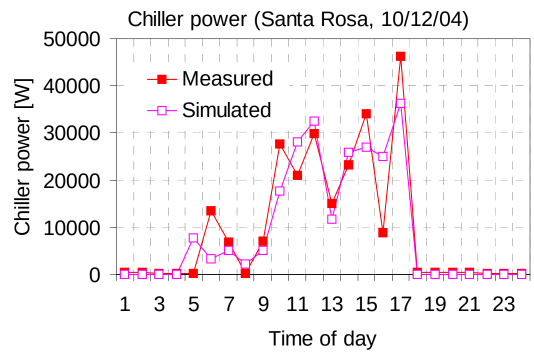

Figure 7 Comparison of simulated and actual chiller power on 10/12/04 for Santa Rosa building

SIMULATION PROCEDURES

ERS Building

The demand-limiting methods were evaluated using the detailed inverse building model for single-day simulations. For parameter estimation with the SA method, data were generated at 15-minute intervals using the inverse model with hourly timesteps and linear interpolation. Outdoor temperatures were generated using statistical correlations from Erbs (1984) with a mean temperature of 90°F and a solar clearness index of 0.8 and actual solar radiation data were used for a clear day in August in Iowa.

For demand-limiting control, precooling was assumed from 7 am to 12 pm at 70°F and then the setpoints were varied from 70°F to 78°F during a demand-limiting period from 12 pm to 6 pm. The base case is night setup control, where setpoint temperatures from 7 am to 6 pm were fixed at 74°F and then reset to 90°F during the other times. For comparison, the demand reduction compared to the base case associated with trajectories determined with the three methods were compared with 'optimal', 'linear-rise', and 'step-up' strategies for adjusting the setpoints. With the 'linear-rise' demand-limiting control strategy, the setpoint was increased linearly from 70°F to 78°F during the demand-limiting period. The 'step-up' demand-limiting strategy involved resetting and maintaining the setpoint at 78°F at the beginning of the demand-limiting period until the end of the period. The 'optimal' demand-limiting strategy used the inverse building model to find demand-limiting setpoint trajectories to yield the minimum peak cooling demand during the demand-limiting period.

Santa Rosa Building

The EnergyPlus model for the Santa Rosa Federal building was used to estimate both cooling load and chiller power for a single day during the on-peak period for the different demand-limiting methods in relation to night setup control. The outdoor temperature for September 24 in 2004 from the site was used and other weather data were taken from TMY data for San Francisco on that day of the year. One day was simulated with different setpoint control methods for hourly time steps. For the SA and ESA methods, data used for parameter estimation were generated at a time interval of 15 minute. Simulations were performed with a time step of 15 minutes but results are presented at hourly time steps.

For demand-limiting control, precooling was assumed from 7 am to 1 pm at 70°F and then the setpoints were varied from 70°F to 78°F during a demand-limiting period from 1 to 5 pm. The base case is conventional control, where setpoint temperatures were fixed at 72°F from 5 am to 5 pm and the zone space temperatures floated at other times. For comparison, the demand reductions compared to the base case associated with trajectories determined with the three methods were compared with 'linear-rise', and the 'step-up' strategies for adjusting the setpoints. Optimization of demand-limiting control was not performed.

Measure of Peak Load Reduction

For the purpose of evaluating performance of the methods in terms of peak cooling demand-reduction, a peak load ratio (PLR) is defined as follows.

$$PLR=\frac{\max\{Q_{dl,k}\}}{\max\{Q_{cc,k}\}} \text{ for } k=1,..,k_{dl} \tag{1}$$

where $Q_{dl,k}$ is cooling load under demand-limiting control and $Q_{cc,k}$ is cooling load under conventional night setup control.

SIMULATION RESULTS

Estimated setpoint trajectories and simulated cooling loads are compared for the SA, ESA, and WA methods.

Parameters of Building Models

Thermal parameters for the SA and ESA methods are estimated using nonlinear regression with actual data. There are two phases associated with the parameter estimation process: a global search and a local search (see Lee and Braun (2004)). For the global search phase, building geometry and thermal properties of air and building materials are used to determine lower and upper bounds of thermal parameters. Bounds on the parameters are estimated as outlined in the following two sections.

Simple building indoor mass model (SA Method)

The shallow mass thermal capacitance can be estimated from:

$$C_{ms}=r_c M_{b,A_{floor}} A_{floor} c_b \tag{2}$$

where A_{floor} = floor area (ft^2), $M_{b,Afloor}$= building mass per floor area (lbm/ft^2), c_b= capacitance of building envelope (Btu/lbm-°F), and r_c= ratio of effective capacitance to building capacitance.

Thermal resistance between the deep mass and shallow mass is approximated as:

$$R_d=d_{b,eff}/\left(k_b A_{sur,ms}\right) \tag{3}$$

where $d_{b,eff}$ = thickness of shallow mass = $r_c d$ (ft), d = effective building thickness (ft), k_b = thermal conductivity of building envelope shallow mass (Btu/hr-ft-F), $A_{sur,ms}$ = $A_{sur,env}$ = surface area of shallow mass, $A_{sur,env}$ = A_{side} + A_{floor} + A_{roof} = envelope surface area, $A_{side}=4[A_{floor}^{1/2} ht_{story} N_{story}(1-r_{A,win,side})]$ = surface area of 4 sides of an effective building having a square shape, N_{story}= building story, ht_{story}= building height per story (ft), $r_{A,win,side}$= ratio of window area to building side surface area, A_{roof} = A_{floor} $(1-r_{A,win,roof})$ = surface area of roof, $r_{A,win,roof}$ = ratio of window to building roof area,

The thermal resistance between the shallow mass and zone air is approximated as:

$$R_s=1/\left(h_i A_{sur,ms}\right) \tag{4}$$

where h_i= inside convection coefficient during the daytime (Btu/hr-ft^2-F).

The thermal resistance between the zone air and outdoor air during the daytime is approximated as:

$$1/R_a=1/R_{win}+1/R_{vent} \tag{5}$$

$$R_{win}=1/(h_i A_{win})+d_{win}/(k_{win} A_{win})+1/(h_o A_{win}) \quad (6)$$

$$R_{vent}=1/\left[\rho_a c_{pa}(V_{vent}+V_{in})\right] \quad (7)$$

where $A_{win}=4(A_{floor}{}^{1/2} ht_{story} N_{story} r_{A,win,side})+A_{floor} r_{A,win,roof}$ = surface area of windows, d_{win}= window thickness (ft), h_o= outside convection coefficient (Btu/hr-ft^2-F), k_{win}= window thermal conductivity (Btu/hr-ft-F), c_{pa}= specific heat of air (Btu/lbm-F), ρ_a= density of air (lbm/ft^3), $V_{vent,person}$= required ventilation flow rate per person (cfm/person), $N_{person,floor}$= people number per 1000ft^2 floor area, $V_{in,volume}$= air exchange rate by infiltration (1/hr), $V_{vent}=V_{vent,person}N_{person,floor}N_{story}$= ventilation flow rate into/out of building (ft^3/hr), V = volume of inside space of building = $A_{floor}ht_{story}N_{story}$ (ft^3), $V_{in}=V_{in,volume}V$= volume flow rate by infiltration (ft^3/hr).

Uncertain parameters that are assigned upper and lower bounds for training are $M_{b,Afloor}$, c_b, r_c, d, k_b, h_i, h_o, $V_{vent,person}$, $N_{person,floor}$, and $V_{in,volume}$.

Simple whole building model (ESA Method)

Thermal capacitance of the effective whole building mass is approximated as:

$$C_m=M_{b,A_{floor}} A_{floor} c_b \ . \quad (8)$$

Thermal resistances between the effective whole building mass and outdoor air, building mass and zone air, and building mass and ground are approximated as:

$$R_o=1/(h_o A_{sur,ms}) \quad (9)$$

$$R_i=1/(h_i A_{sur,ms}) \quad (10)$$

$$R_g=c_g/A_{floor} \quad (11)$$

where c_g = thermal contact factor and a range of 2 to 5 was assumed.

Thermal resistance between the zone air and outdoor air is approximated in the same way as for the simple indoor mass model.

ERS Building Results

Table 1 in Appendix A gives numerical bounds for the building parameters used in training the simple ERS building models associated with the SA and ESA methods. Upper and lower bounds for simplified model parameters, estimated results for parameters, and predicted peak demand for the SA and ESA methds are listed in Table 3 and Table 4 in Appendix B.

Figure 8 compares setpoint trajectories during the demand-limiting period for the different setpoint control methods. In this figure, NS denotes night-setup control with a constant setpoint temperature of 74°F. The demand-limiting setpoint trajectories obtained with the WA, ESA, SA, and optimal methods are between the step-up and linear-rise strategies.

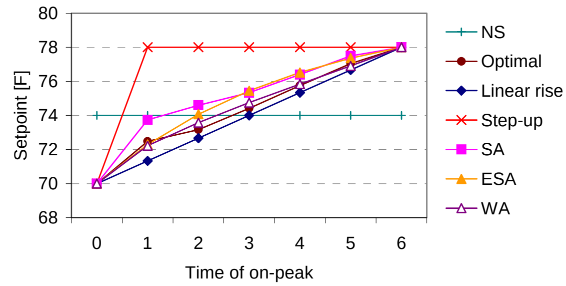

Figure 8 Comparison of setpoint trajectories for different setpoint control methods during the demand-limiting period in the ERS building

Figure 9 compares PLR (peak load ratio) for the different setpoint control methods. 'Optimal' demand-limiting gives the lowest PLR of 0.71 while the WA, ESA, and SA methods gave PLR values in the range of 0.72 to 0.77, which are within 10% of the optimal method. All of the trajectories determined with these methods perform significantly better than the 'step-up' and 'linear-rise' setpoint control methods in terms of peak load reduction. The results in Figure 9 for the WA, ESA, and SA methods include both simulation and predicted PLR values. The predicted PLRs were determined using the SA, ESA, and WA methods, whereas the simulated values were determined with the detailed inverse model after application of the trajectories determined by the methods. The WA method provides the lowest simulated PLR values and also the best predictions for PLR. The SA method has the worst performance and ability to predict the PLR. The SA method over-predicts the PLR because it utilizes a deep mass temperature determined for conventional night setup control.

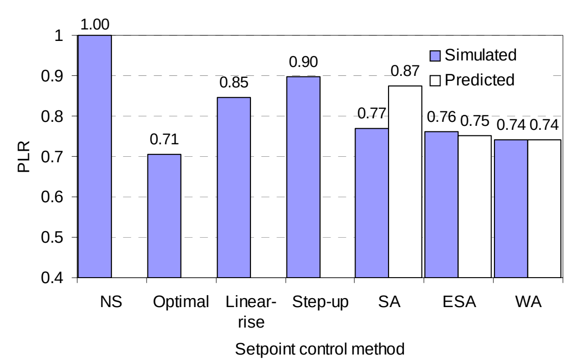

Figure 9 Comparison of peak load ratio for different setpoint control methods in the ERS building

Figure 10 presents cooling load variations during the demand-limiting peak period for the different control strategies. Note that the hour labeled "0" is the hour prior to the start of the demand-limiting period and has loads that are greater than the demand-limiting period for most of the strategies. The shape of the profile is sensitive to the variation in setpoints. The optimal and near-optimal strategies provide "flat" load profiles.

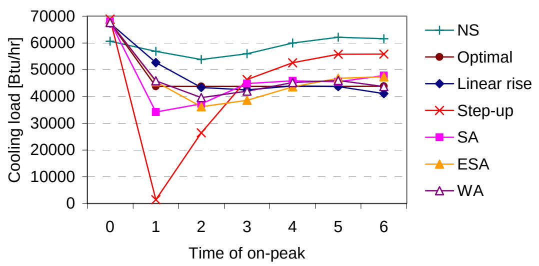

Figure 10 Comparison of simulated cooling load during the demand-limiting period in the ERS building

Santa Rosa Building Results

Table 2 in Appendix A gives numerical bounds for the building parameters used for training the Santa Rosa building models associated with the SA and ESA methods. Upper and lower bounds for simplified model parameters, estimated results for parameters, and predicted peak demand for the SA and ESA methods are listed Table 5 and Table 6 in Appendix B.

Figure 11 compares setpoint trajectories during the demand-limiting period for different setpoint control methods. NS denotes the conventional control with night-setup having a constant setpoint temperature of 72°F. Once again, the demand-limiting setpoint trajectories are located between the step-up and linear-rise strategies. Figure 12 compares PLR for the different setpoint control methods. The cooling demand reduction potential is between 0.56 and 0.60 for the WA, ESA, and SA methods. All three methods worked extremely well for this case and perform better in terms of cooling demand reduction compared to the 'step-up' and 'linear-rise' setpoint control methods. In addition, all the methods accurately predicted the PLR. Compared to the predicted PLR for the small ERS building shown in Figure 9, the PLR prediction of the SA method for the large building model resulted in better performance. When predicting the PLR using the SA method, the deep mass temperature for conventional control is assumed for demand-limiting control. Based on these simulation results, it is thought that the deep mass temperature for a large building varies less with control strategy than for small buildings.

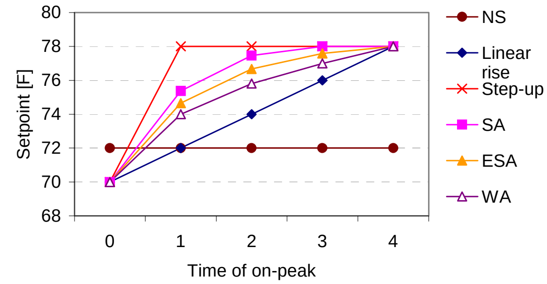

Figure 11 Comparison of setpoint trajectories for different setpoint control methods during the demand-limiting period for the Santa Rosa building

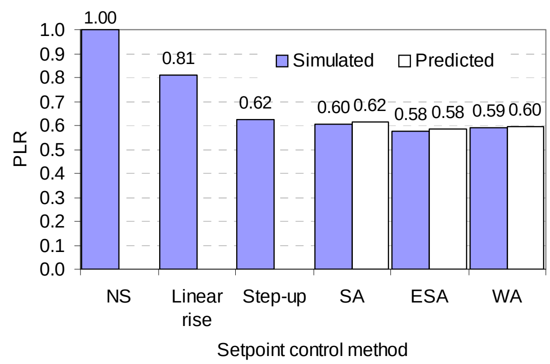

Figure 12 Comparison of peak load ratio for different setpoint control methods for the Santa Rosa building

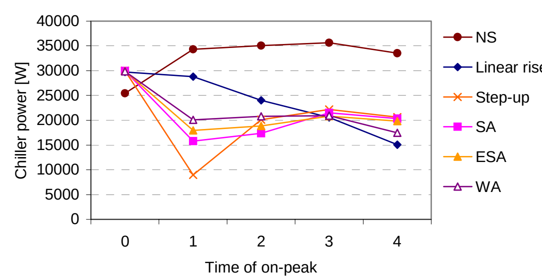

Figure 13 Comparison of chiller power for different setpoint control methods for the Santa Rosa building

Figure 13 shows chiller power variations during the demand-limiting period for the different strategies. The WA, ESA, and SA methods all yield relatively "flat" profiles compared to the conventional and ad-hoc strategies. It should be noted that the linear-rise strategy worked relatively well for the ERS building, but not for the Santa Rosa building. This result reinforces the importance of determining a site-specific strategy. It is also noted that the step-up strategy showed as good performance as the three demand-limiting controls in terms of peak demand reduction.

CONCLUSIONS

The SA, ESA, and WA methods developed in a companion paper (Lee and Braun 2006b) were tested through simulation for buildings representative of small (ERS) and large (Santa Rosa) commercial sites. For the ERS building, simulated peak load reductions for all three methods were 23 to 26% and were within about 10% of the maximum possible peak load reduction of 29% associated with optimal control for a 6-hour demand-limiting period. The simulated peak chiller power demand was reduced by more than 40% for all three methods for the Santa Rosa building for a 4-hour demand-limiting period.

For future work, robustness of the simplified demand-limiting methods should be investigated since all driving environmental conditions were assumed to be the same for training and demand-limiting days in this study. The impact of different weather conditions and duration of data for training should be studied.

NOMENCLATURE

PLR = peak load ratio defined as ratio of peak load under demand-limiting control to peak load under conventional control

k_{dl} = length of demand-limiting period

REFERENCES

Erb, D.G. 1984. Models and Applications for Weather Statistics Reltated to Building Heating and Cooling Loads, Ph.D. Thesis, University of Wisconsin at Madison.

Lee, K.-H. and Braun, J.E. 2004. Development and Application of an Inverse Building Model for Demand Response of Small Commercial Buildings, Submitted for Review, SimBuild 2004 IBPSA-USA Conference, University of Colorado.

Lee, K.-H. and Braun, J.E. 2006a. An Experimental Evaluation of Demand-Limiting Using Building Thermal Mass in a Small Commercial Building, ASHRAE Transactions, Vol.112, Pt.1.

Lee, K.-H. and Braun, J.E. 2006b. Development of Methods for Determining Demand-Limiting Setpoint Trajectories in Commercial Buildings Using Short-Term Data Analysis, SimBuild 2006 IBPSA-USA National Conference, MIT.

US Department of Energy, 2005. ENERGYPLUS™, Input Output Reference.

Xu, P., Haves, P., Zagreus L. and Piette M. Demand Shifting with Thermal Mass in Large Commercial Buildings (Field Tests, Simulation and Results)", Lawrence Berkeley National Laboratory, CEC-500-2006-009, January 2006.

APPENDICES

Appendix A: Upper and Lower Bounds for Building Parameters

Table 1 Upper and lower bounds for ERS building parameters

Building parameters	Min	Max	Fixed
A_{floor} (ft^2)	-	-	2200
N_{story} (#)	-	-	1
ht_{story} (ft)	-	-	8.5
$r_{A,win,side}$ (-)	-	-	0.562
$r_{A,win,roof}$ (-)	-	-	0
d_{win} (ft)	-	-	0.1
k_{win} (Btu/hr-ft-°F)	-	-	0.8089
ρ_a (lbm/ft^3)	-	-	0.07433
c_{pa} (Btu/lbm-°F)	-	-	0.2404
$M_{b,A_{floor}}$ (lbm-ft^2)	30	50	-
c_b (Btu/lbm-°F)	0.1	0.3	-
r_c (-)	0.1	0.3	-
d (ft)	0.5	1	-
h_i (Btu/hr-ft^2-°F)	0.4	0.8	-
h_o (Btu/hr-ft^2-°F)	2	4	-
k_b (Btu/hr-ft-°F)	0.1	0.4	-
$V_{vent,person}$ (cfm/person)	13	18	-
$N_{person,floor}$ (people/1000ft^2)	1e-9	1e-9	-
$V_{in,volume}$ (1/hr)	0.0	0.001	-

Table 2 Upper and lower bounds for Santa Rosa building parameters

BUILDING PARAMETERS	MIN	MAX	FIXED
A_{floor} (ft^2)	-	-	20000
N_{story} (#)	-	-	3
ht_{story} (ft)	-	-	13.0
$r_{A,win,side}$ (-)	-	-	0.4
$r_{A,win,roof}$ (-)	-	-	0
d_{win} (ft)	-	-	0.02
k_{win} (Btu/hr-ft-°F)	-	-	0.52
ρ_a (lbm/ft^3)	-	-	0.07433
c_{pa} (Btu/lbm-°F)	-	-	0.2404
$M_{b,A_{floor}}$ (lbm-ft^2)	30	50	-
c_b (Btu/lbm-°F)	0.1	0.3	-
r_c (-)	0.1	0.3	-
d (ft)	0.5	2	-
h_i (Btu/hr-ft^2-°F)	0.4	0.8	-
h_o (Btu/hr-ft^2-°F)	2	4	-
k_b (Btu/hr-ft-°F)	0.1	0.4	-
$V_{vent,person}$ (cfm/person)	15	25	-
$N_{person,floor}$ (people/1000ft^2)	1	5	-
$V_{in,volume}$ (1/hr)	0.0	0.001	-

Appendix B: Bounds and Estimated Results for Parameters in the SA and ESA Methods

Table 3 Bounds and estimated results for parameters and predicted peak demand for SA method applied to ERS building

PARAMETERS	LOWER BOUND	UPPER BOUND	ESTIMATED OR PREDICTED
C_{ms} [Btu/°F]	707	9607	2190.3
R_d [Btu/°F-hr]	2.0E-5	5.2E-4	4.37E-4
R_s [Btu/°F-hr]	2.0E-4	4.8E-4	2.23E-4
R_a [Btu/°F-hr]	3.0	32.8	5.48
g [Btu/hr]	$-Q_{z,cc,min}$	$Q_{z,cc,min}$	-26983.4
g_t [hours]	0.01	1.0	0.26
$T_{dm,cc}$ [°F]	74.0	95.1	82.8
$Q_{g,c}$ [Btu/hr]	$0.4Q_{z,cc,min}$	$0.6Q_{z,cc,min}$	24208.5
$Q_{z,dl}$ [Btu/hr]	-	-	54324.94

Table 4 Bounds and estimated results for parameters and predicted peak demand for ESA method applied to ERS building

PARAMETERS	LOWER BOUND	UPPER BOUND	ESTIMATED OR PREDICTED
C_{ms} [Btu/°F]	3466	32141	16102.2
R_o [Btu/°F-hr]	1.7E-4	6.2E-3	6.02E-3
R_i [Btu/°F-hr]	2.4E-4	4.8E-4	1.24E-4
R_a [Btu/°F-hr]	3.3	32.8	4.22
R_g [Btu/°F-hr]	9.0E-4	2.3E-3	2.33E-3
τ [hours]	-	-	3.94
$minQ_{z,dl,max}$ [Btu/hr]	-	-	46696.8

Table 5 Bounds and estimated results for parameters and predicted peak demand for SA method applied to Santa Rosa building

PARAMETERS	LOWER BOUND	UPPER BOUND	ESTIMATED OR PREDICTED
C_s [Btu/°F]	19301	262033	59756.3
R_d [Btu/°F-hr]	2.7E-6	10.0E-5	1.9E-5
R_s [Btu/°F-hr]	2.3E-5	4.6E-5	2.7E-5
R_a [Btu/°F-hr]	4.0E-2	0.15	0.141
g [Btu/hr]	$-Q_{z,cc,min}$	0	-23523.05
g_t [hours]	0.01	2.0	1.50
$T_{dm,cc}$ [°F]	72.0	85.83	80.07
$Q_{g,c}$ [Btu/hr]	$0.1Q_{z,cc,min}$	$0.5Q_{z,cc,min}$	56465.31
$Q_{z,dl}$ [Chiller,W]	-	-	22467.00

Table 6 Bounds and estimated results for parameters and predicted peak demand for ESA method applied to Santa Rosa building

PARAMETERS	LOWER BOUND	UPPER BOUND	ESTIMATED OR PREDICTED
C_m [Btu/°F]	94536	876586	115480.4
R_o [Btu/°F-hr]	1.5E-6	5.4E-4	5.23E-4
R_i [Btu/°F-hr]	2.4E-6	4.6E-5	2.0E-5
R_a [Btu/°F-hr]	4.0E-2	0.15	4.3E-2
R_g [Btu/°F-hr]	1.0E-4	2.5E-4	2.45E-4
τ [hours]	-	-	1.24
$minQ_{z,dl,max}$ [Chiller,W]	-	-	21581.37